A study of phase transition in $(NH_4)_3WO_3F_3$ oxyfluoride by Raman scattering

A. S. Krylov[1], **J. V. Gerasimova**[*, 1], **A. N. Vtyurin**[**, 1], **V. D. Fokina**[1], **N. M. Laptash**[2] and **E. I. Voyt**[2]

[1] Kirensky Institute of Physics, 660036 Krasnoyarsk, Russia
[2] Institute of Chemistry, 690022 Vladivostok, Russia

Raman scattering spectra of perovskite-like $(NH_4)_3WO_3F_3$ oxyfluoride are studied in the $70–3600$ cm^{-1} frequency range and the $93–323$ K temperature range including the transition point from orientationally disordered cubic phase into the lower symmetry one. Internal vibrations of ammonium ions and WO_3F_3 octahedra have been found to exhibit transition anomalies. Analysis of measurements suggests that the transition under study is due mainly to the ordering of octahedra.

1 Introduction

Perovskite-like fluorites A_3BX_6 (A and B are metal cations, X are halogens or oxygen ions) belong to the cryolite-elpasolite family [1] with a cubic high-temperature phase ($Fm\bar{3}m$ space group, $Z = 4$). According to [2], mixed $A_3BO_xHal_{(6-x)}$ compounds (x depends on A and B valences) retain the same cubic symmetry of the-high symmetry phase (see Fig. 1); oxygen and halogen ions are distributed statistically over the crystal lattice and the local symmetry of $BO_xHal_{(6-x)}$ octahedra is lower than the cubic one [3, 4].

On cooling, these fluorides and oxyfluorides undergo phase transition sequences, which may be related to ordering of octahedron ions [1, 5, 6]. The resulting distorted phases may be of different nature – ferroelastic phases are more typical for fluorides while oxyfuorides are known to have both ferroelectric and ferroelastic ones.

Substitution of metal cations for ammonium ions results in additional structural disorder due to orientational degrees of freedom of ammonium tetrahedrons. Moreover, O_h symmetry of one of the cation positions is inconsistent with a tetrahedron structure, and the corresponding ammonium will be orientationally disordered in the cubic phase.

Studies of phase transitions in ammonium oxyfluorides are in the initial stage only [6]. Here we present results of Raman scattering study for $(NH_4)_3WO_3F_3$ crystal.

2 Experimental

Ammonium oxyfluoride $(NH_4)_3WO_3F_3$ was synthesized from $(NH_4)_2WO_2F_4$ hot solution with excessive NH_4F and subsequent addition of NH_4OH solution. Small colorless transparent octahedral crystals precipitated; after spontaneous crystallization they grew to about 40 μm. The detailed procedure is given in

[*] Corresponding author: e-mail: jul@iph.krasn.ru, Phone: +7 3912 432 635, Fax: +7 3912 438 923
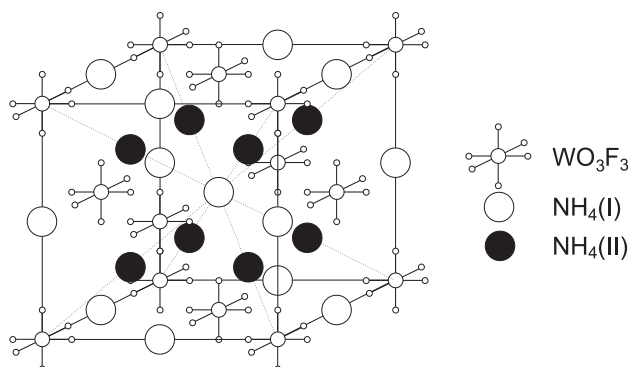[**] e-mail: vtyurin@iph.krasn.ru, Phone: +7 3912 494 294, Fax: +7 3912 438 923

Fig. 1 Unit cell of the cubic phase of a $(NH_4)_3WO_3F_3$ crystal. Ammonium cations are disordered orientationally and are shown as spheres. Oxygen and fluorine positions in WO_3F_3 octahedra are also unknown.

[6]. X-ray powder diffraction confirms their cubic structure ($Fm\overline{3}m$, $a = 0.9156$ nm); the diffraction pattern revealed no extra peaks of initial components or foreign phases.

Raman spectra in the backscattering geometry were recorded with RFS-100/S Fourier-Raman spectrometer (Bruker) over the range $70-3600$ cm^{-1} with 1 cm^{-1} resolution under continuous Nd:YAG laser excitation (1.06 μm, 350 mW); spectra have been averaged over 400 scans. Microcrystals were placed in a quartz-covered steel container; temperature measurements were made with Specac optical cryostat providing $83-523$ K temperatures with 0.1 K precision.

The data were processed with Peak Fit and Sigma Plot 8.0 software packages (both SPSS Inc.); line contours were interpolated with Voight and dispersive functions (with account of the Bose–Einstein factor).

3 Experimental results

3.1 General structure of spectrum

The experimental spectrum of $(NH_4)_3WO_3F_3$ microcrystals at room temperature is shown in Fig. 2. Four regions readily stand out here.

Regions at $2700-3500$ cm^{-1} and $1200-1600$ cm^{-1} have two lines each corresponding to stretching and deformation internal modes of ammonium ions, respectively. The lines here are rather broad, but are not split. Their positions: 2770 cm^{-1} and 3092 cm^{-1} for stretching modes, 1489 cm^{-1} and 1697 cm^{-1} for de-
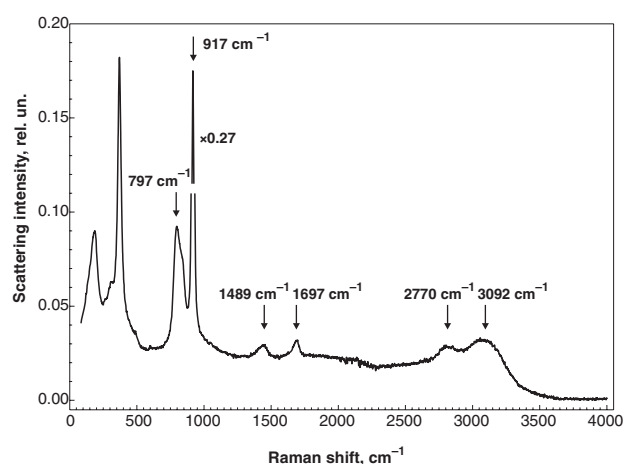

Fig. 2 Raman spectra of $(NH_4)_3WO_3F_3$ at room temperature.

Table 1 Quantum-chemical (ECP/SBKJC/B3LYP) simulations for vibrational spectra of $WO_3F_3^{3-}$ ions.

irreducible representation	frequency, cm^{-1}	relative Raman intensity
cis-conformation, C_{3v}		
A_1	915	37.1
E	821	4.7
A_1	415	3.7
E	342	0.3
A_1	336	0.3
E	334	1.7
A_1	274	0.3
E	252	0.2
E	175	0.3
A_2	137	0.0
trans-conformation, C_{2v}		
A_1	887	12.4
A_1	810	13.6
B_1	745	0.5
A_1	455	4.9
B_2	433	0.0
B_1	358	0.7
A_1	328	1.1
A_2	292	0.0
B_1	308	1.1
A_1	263	3.9
B_2	256	0.8
B_2	229	0.4
B_1	211	0.6
A_1	151	2.6
B_2	0.35	0.0

formation ones – are quite close to free-ion frequencies (3040 cm^{-1}, 3145 cm^{-1}, 1400 cm^{-1} and 1680 cm^{-1}, according to [7]). A small shift of these lines and no splitting (either positional or due to degeneracy removal for *E* and *F* modes) indicate weak distortion of ammonium ions by the crystal environment and their feeble interactions with each other.

The 750–1000 cm^{-1} region includes longitudinal vibrations of W–O bonds of $WO_3F_3^{3-}$ ions. To interpret them we performed quantum-chemical simulation of two possible configurations of these ions: *cis*-$WO_3F_3^{3-}$ of C_{3v} symmetry and the *trans*-$WO_3F_3^{3-}$ of C_{2v} one. Calculations were done within the limited Hartree–Fock approach with the B3LYP density functional. For W, F, O atoms we used the standard SBKJC basis [8] together with a pseudorelativistic core potential supplemented with two diffuse functions. Simulations were performed with 16 processors MBC-1000 Linux-cluster by the GAMESS [9] program package. Mechanical optimization of the ionic geometry resulted in overestimated interatomic distances (as compared with experimental X-ray data); so, first, we simulated the $[Na_6WO_3F_3]^{3+}$ cluster and used this ionic geometry for dynamical simulations. A more detailed description of this procedure is given in [10]. Frequencies produced and relative Raman intensities for two ionic configurations are given in Table 1.

The position of the most intense line at 917 cm^{-1} actually coincides with the calculated frequency 915 cm^{-1} of the A_1 vibration (W–O stretches) for the *cis*-conformation of the octahedron. The complex
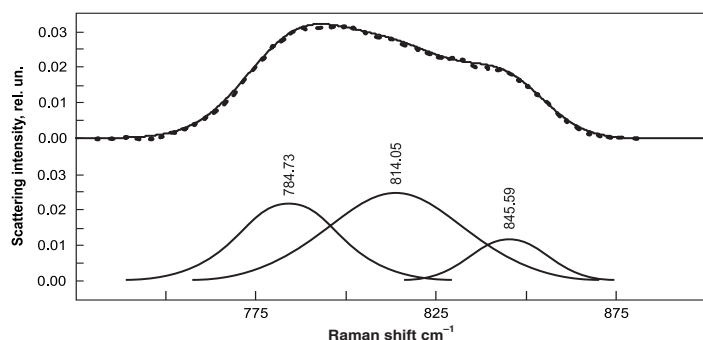
Fig. 3 Deconvolution of $775-850$ cm^{-1} band at 232 K into three components. Dotted line at the top is the experimental spectrum; continuous line is the result of the deconvolution procedure. Voight components are shown at the bottom; their parameters (position/HWHH, in cm^{-1}) are: $784.72/16.74 - 814.04/22.69 - 845.59/12.80$.

band at 775–850 cm^{-1} is close to the doubly degenerate WO_3 stretching mode for the same configuration (calculated frequency is 821 cm^{-1}). The relative intensities of these two lines correlate reasonably with predicted values as well (see Table 1). The two predicted Raman lines of W–O stretches for *trans*-conformation have lower frequencies and comparable intensities – so we can conclude that the *cis*-conformation of $WO_3F_3^{3-}$ octahedra is likely to be more preferable. Our attempts to deconvolute 775–850 cm^{-1} into Voight or dispersive components (Fig. 3) showed it to include at least three individual lines: 784 cm^{-1}, 814 cm^{-1} and 845 cm^{-1}. This triplet may include two lines of split degenerated E mode of *cis*-conformation and most intense A_1 mode of the *trans*-conformation of $WO_3F_3^{3-}$ octahedra (see Table 1).

One more line of the W–O stretching vibration for the *trans*-conformation, not so intense yet Raman active, is predicted at 887 cm^{-1}. The experimental Raman signal increases there slightly, but not so much as to interpret it as a spectral line with confidence.

The area below 500 cm^{-1} corresponds to stretching vibrations of W–F bonds and deformation modes of $WO_3F_3^{3-}$ ions. Their experimental frequencies are in fairly good agreement with calculated values [10] for the *cis*-conformation of $WO_3F_3^{3-}$ octahedra too, so it is safe to conclude that in the studied crystal these ions are mainly in the *cis*-conformation with some conformational dynamics.

3.2 Temperature transformation of spectrum

The spectra produced vary slightly on cooling to 200 K, except for a minor natural decrease of line widths. At 200 K (at the phase transition point found by X-ray and heat capacity measurements [6]) and below the spectrum drastically changes.

In the regions of ammonium internal modes the scattering intensity grows considerably (Fig. 4); single separated lines are replaced by complex structural bands. The intensity of these bands increases further on cooling to 90 K, while their widths remain very large (typical WHHs are above 100 cm^{-1}).

The region of stretching W–O vibrations undergoes considerable changes, too. The most intense line at 917 cm^{-1} narrows sharply and splits into a doublet (Fig. 5). Figure 6 demonstrates the temperature dependences of frequencies and widths of the resulting doublet – the damping anomaly at the transition point is apparent here. At the same time, away from the transition these widths are practically constant (in contrast to the well-ordered elpasolite crystals – see, e.g., [11] for Rb_2KScF_6) – evidently this damping is not related to vibrational anharmonicity.

The 775–850 cm^{-1} band undergoes similar changes (Fig. 7). As close as $1-2$ K below the transition point its components narrow considerably and all three of them are seen clearly. Further cooling splits each of them into a doublet, their components continue to slide apart and narrow slightly (Fig. 8).

Similar, though not so drastic changes (line narrowing and new lines appearance) take place in the lower-frequency part of the spectrum (Fig. 9).
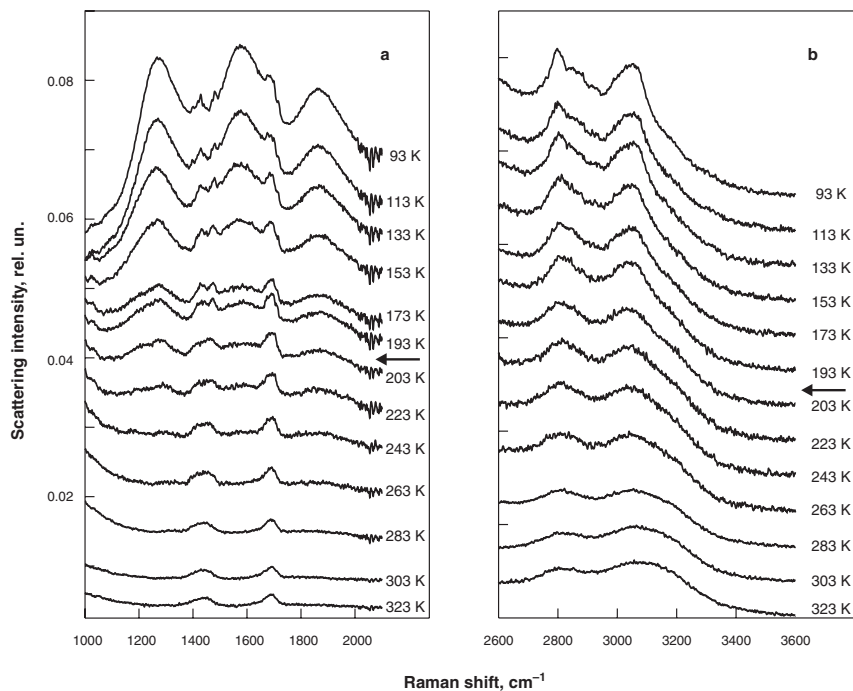
Fig. 4 Temperature transformation of ammonium internal modes. (a) is the deformation and (b) are stretching vibrations. Phase transition temperature is shown by arrows.
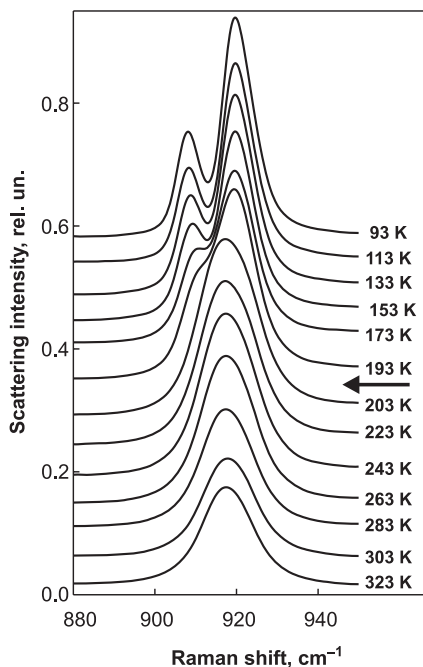

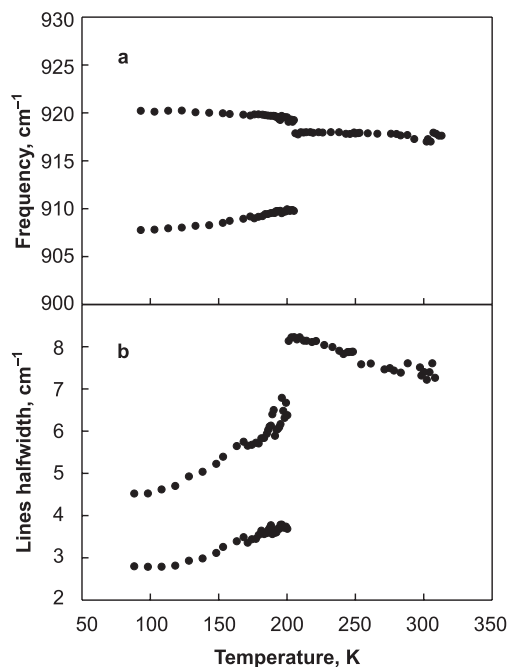**Fig. 5** Splitting of the 917 cm⁻¹ line at the phase transition.

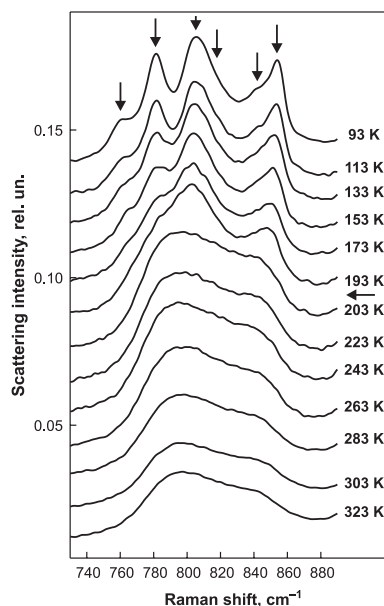**Fig. 6** Temperature dependences of frequency (a) and HWHH (b) for components of the 917 cm⁻¹ doublet.

Fig. 7 Transformation of $775-850$ cm^{-1} band with temperature. Positions of deconvoluted components are shown with arrows.
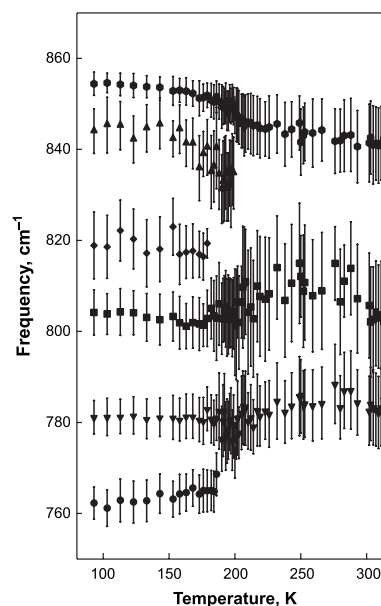
Fig. 8 Temperature dependences of these deconvoluted components positions (for Voight contours).

It is obvious that the observed evolution of the spectrum is due to the orientational ordering of molecular ions at the phase transition – earlier it was mentioned that both ammonium cations and $WO_3F_3^{3-}$ octahedra in the cubic phase are disordered. Sharp narrowing of W–O lines evidences that anions are ordering at the transition. Yet ammonium cations remain disordered like the widths of their internal modes. Interaction of cations with an ordered anion sublattice strengthens to distort them (ammonium-protons and oxygens of anion sublattice can be suggested to develop hydrogen bonds) and complicates
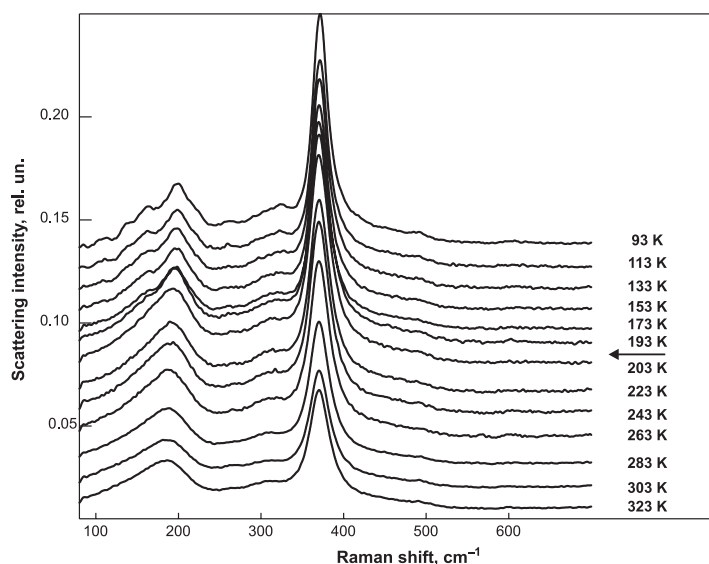

Fig. 9 Temperature transformation of the spectrum in the low-frequency range.

the upper part of the spectra. It seems that these interactions partly remain even in the disordered cubic phase – these extra lines of ammonia deformations are slightly visible just above the transition point (Fig. 4a).

4   Conclusion

So the full spectrum of $(NH_4)_3WO_3F_3$ crystal within the $93-323$ K temperature range has been obtained and analyzed for the first time, lines of ammonium stretching and deformation modes as well as $W-O$ bond vibrations of $WO_3F_3^{3-}$ anions have been identified.

The experimental spectrum of $WO_3F_3^{3-}$ internal modes as compared with quantum-chemical simulations confirms that these anions are mainly found in the *cis*-conformation.

All molecular ions in the cubic phase are disordered orientationally, this is evidenced by wide internal lines and the weak temperature dependence of these widths away from the transition point.

Cooling below the transition point orders the anionic sublattice orientationally, this manifests in substantial narrowing of $W-O$ vibration lines. Strong interaction of ammonium ions with ordering anion sublattice leads to their distortions, this is proved by the splitting and growing intensity of ammonium internal lines; however, ammonium ions remain disordered.

References

[1] I. N. Flerov, M. V. Gorev, K. S. Aleksandrov, A. Tressaud, J. Grannec, and M. Cousi, Mater. Sci. Eng. R **24**, 81 (1998).
[2] G. von Pausewang and W. Rüdorff, Z. Anorg. Allg. Chem. **364**, 69 (1969).
[3] K. von Dehnicke, G. Pausewang, and W. Rüdorff, Z. Anorg. Allgem. Chem. **366**, 64 (1969).
[4] M. Couzi, V. Rodriguez, J.-P. Chaminade, M. Fouad, and J. Ravez, Ferroelectrics **80**, 109 (1988).
[5] I. N. Flerov, M. V. Gorev, S. V. Melnikova, S. V. Misul, V. N. Voronov, and K. S. Aleksandrov, Phys. Solid State **34**, 2185 (1992).
[6] I. N. Flerov, M. V. Gorev, V. D. Fokina, A. F. Bovina, and N. M. Laptash, Phys. Solid State **46**, 915 (2004).
[7] K. Nakamoto, in: Infrared and Raman Spectra of Inorganic and Coordination Compounds. A Wiley Interscience Publication (John Wiley and Sons, New York, 1986).
[8] W. J. Stevens, H. Basch, M. Krauss, and P. Jasien, Can. J. Chem. **70**, 612 (1992).
[9] M. W. Schmidt, K. K. Baldridge, J. A. Boatz, and S. T. Elbert, J. Comput. Chem. **14**, 1347 (1993).
[10] N. M. Laptash, L. A. Sheludyakova, T. V. Basova, and E. I. Voit, in: 14th European Symposium on Fluorine Chemistry. Book of Abstracts (Poznan, Poland, 2004) p. 328. Accepted for publication in J. Fluorine Chem. (2005).
[11] S. N. Krylova, A. N. Vtyurin, A. Bulou, A. S. Krylov, and N. G. Zamkova, Phys. Solid State **46**, 1311 (2004).